Highlights from the Pierre Auger Observatory: Composition and Anisotropy

M. Unger (KIT)

Solvay Workshop, SuGAR 2018, Brussels

Introduction

The Pierre Auger Observatory

The Pierre Auger Observatory

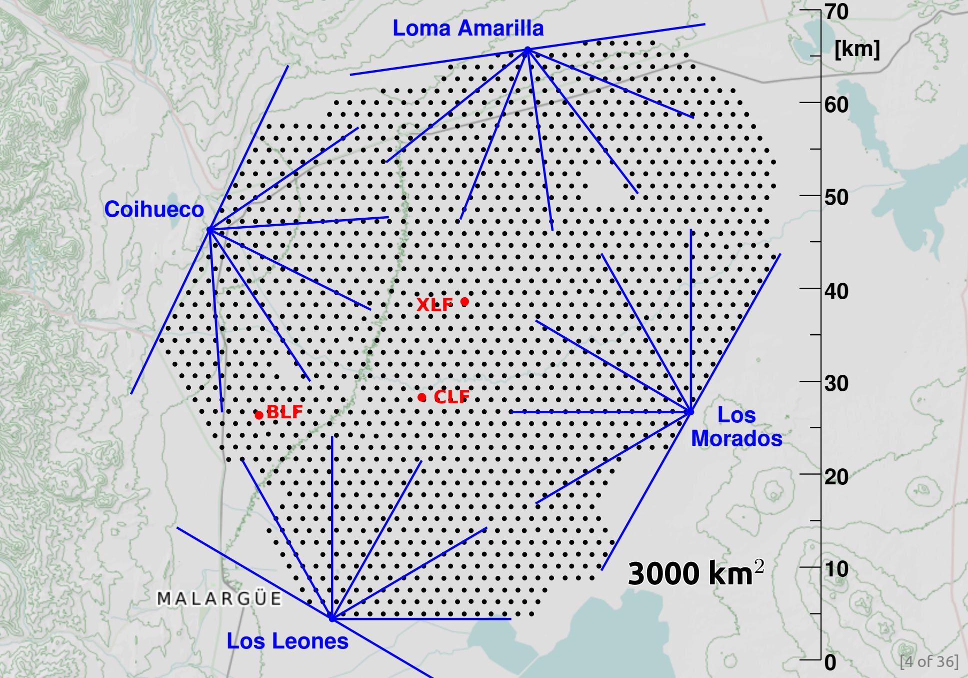

The Pierre Auger Observatory

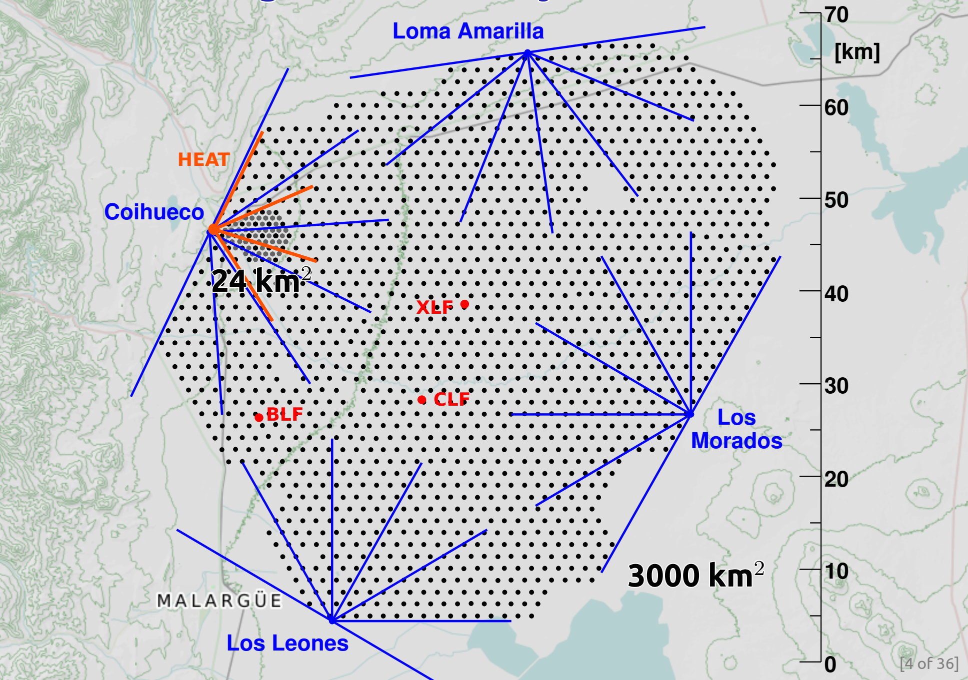

The Pierre Auger Observatory

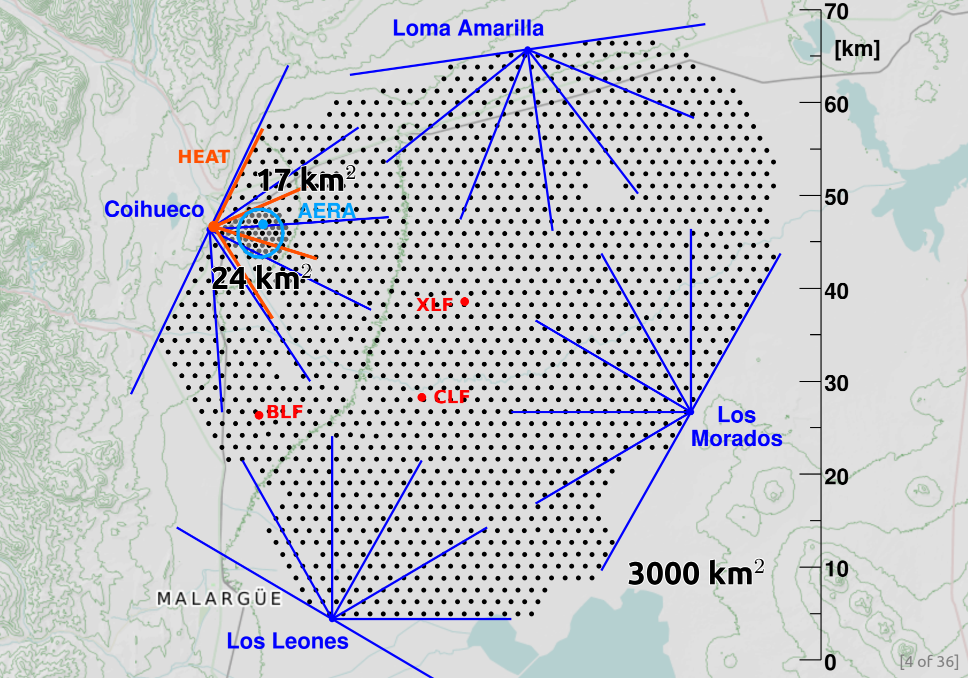

UHE Exposure

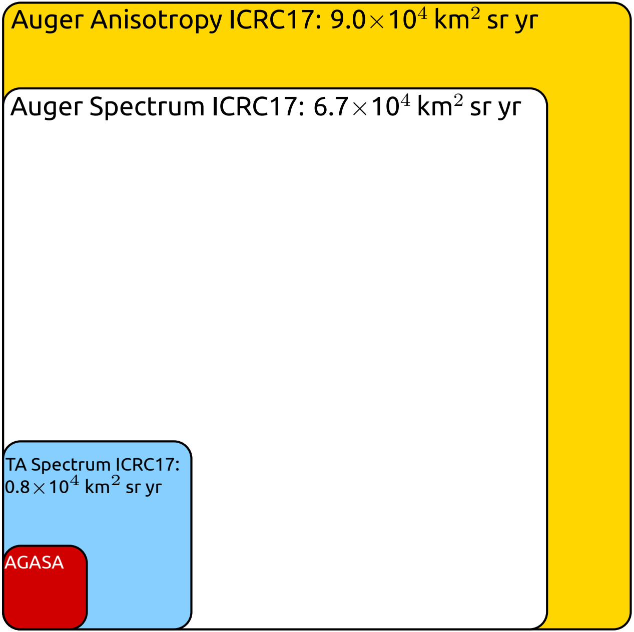

Hybrid Detection of Air Showers

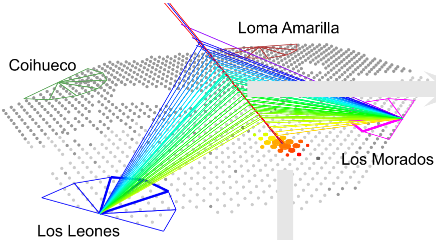

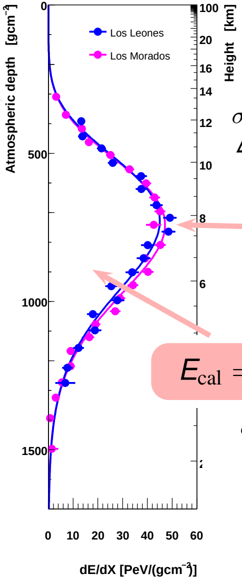

$\sigma_{X_\mathrm{max}} \lesssim 20\,\mathrm{g/cm^2}$
$\Delta_\mathrm{sys} \lesssim 10\,\mathrm{g/cm^2}$

X_max

$E_\mathrm{cal} = \int \frac{\mathrm{d}E}{\mathrm{d}X}\,\mathrm{d}X$

$\sigma_E/E \sim 8\,\%$
$\Delta_\mathrm{sys} \approx 15\,\%$

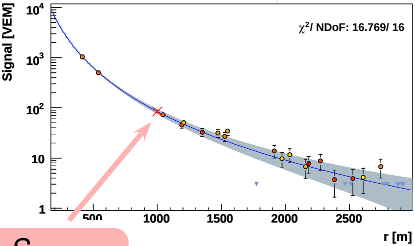

S_{1000}

$E_\mathrm{surface} = f(S_{1000},\ \theta)$

Energy Calibration

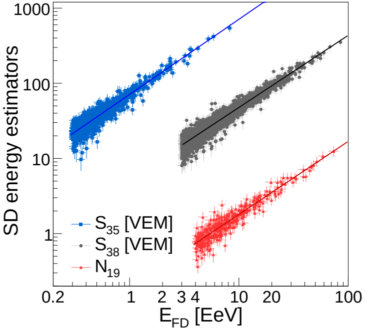

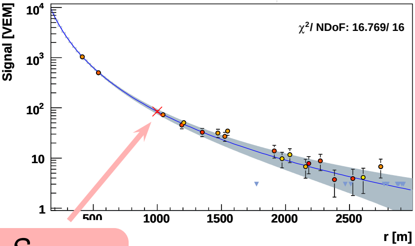

S_{1000}

$E_{\mathrm{surface}} = f(S_{1000},\, \theta)$

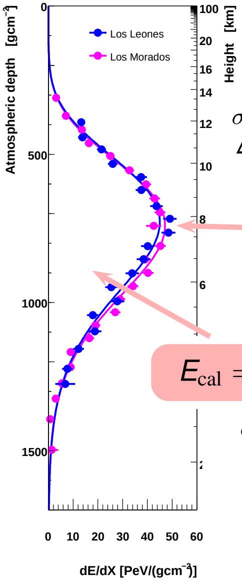

$\sigma_{X_{\mathrm{max}}} \lesssim 20\,\mathrm{g/cm^2}$
$\Delta_{\mathrm{sys}} \lesssim 10\,\mathrm{g/cm^2}$

X_{max}

$E_{\mathrm{cal}} = \int \frac{\mathrm{d}E}{\mathrm{d}X}\,\mathrm{d}X$

$\sigma_E/E \sim 8\,\%$
$\Delta_{\mathrm{sys}} \approx 15\,\%$

Energy Spectrum

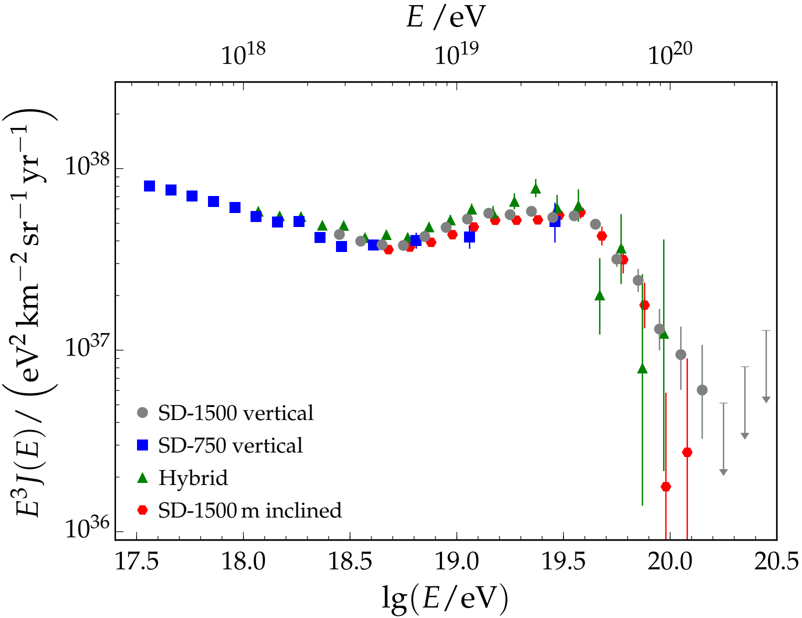

Combined Energy Spectrum

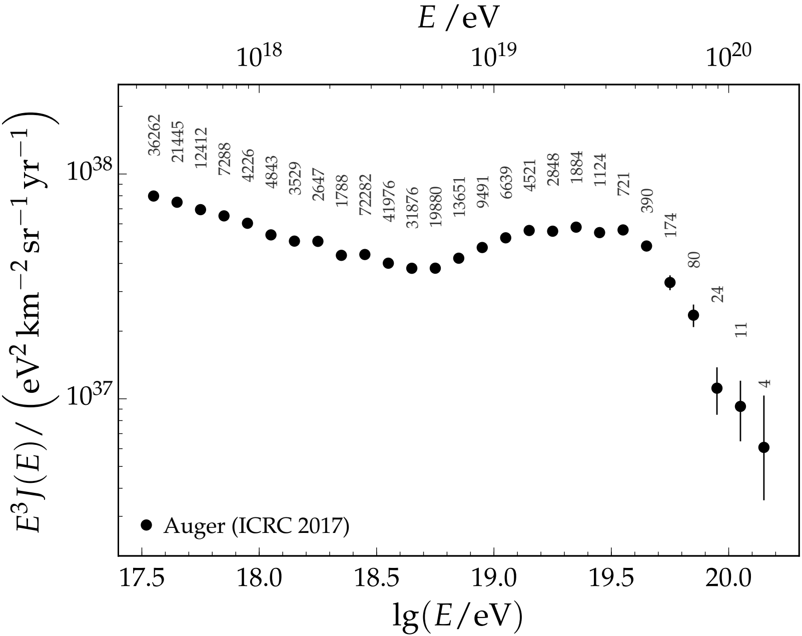

Combined Energy Spectrum

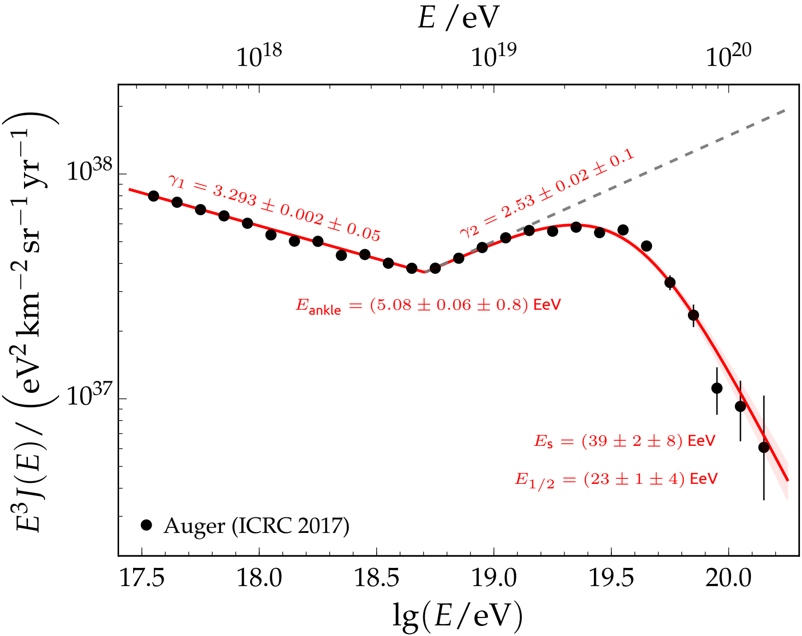

Mass Composition

X_{max}

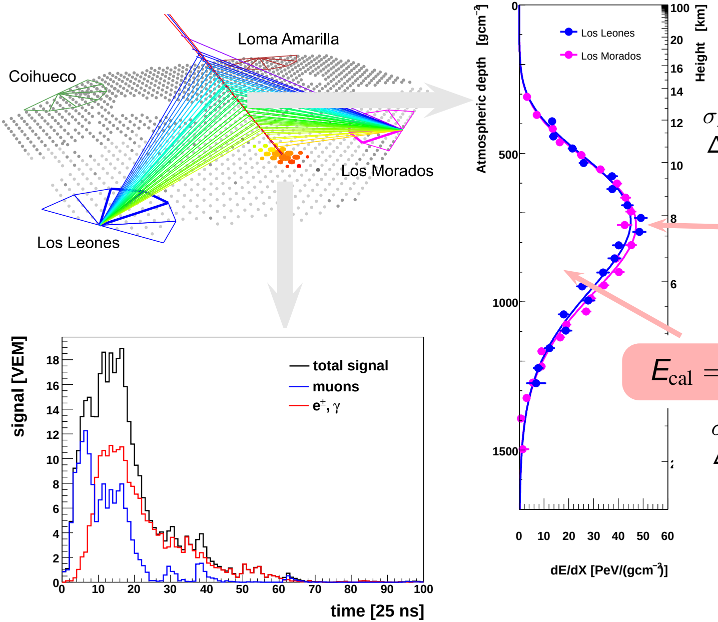

$\sigma_{X_{\rm max}} \lesssim 20\,{\rm g/cm^2}$

$\Delta_{\rm sys} \lesssim 10\,{\rm g/cm^2}$

$X_{\rm max}$

$$E_{\rm cal} = \int \frac{dE}{dX}\, dX$$

$\sigma_E/E \sim 8\,\%$

$\Delta_{\rm sys} \approx 15\,\%$

X_{max}

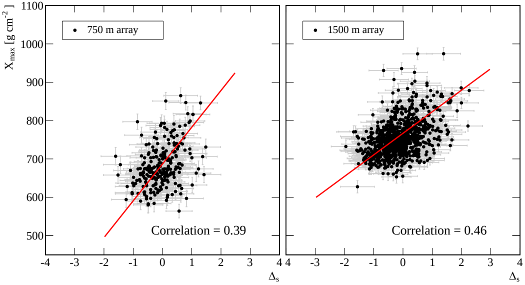

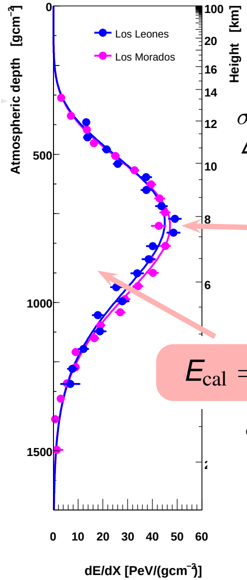

$\sigma_{X_{max}} \lesssim 20\,\mathrm{g/cm^2}$
$\Delta_{sys} \lesssim 10\,\mathrm{g/cm^2}$

X_{max}

$E_{cal} = \int \frac{\mathrm{d}E}{\mathrm{d}X}\,\mathrm{d}X$

$\sigma_E/E \sim 8\,\%$
$\Delta_{sys} \approx 15\,\%$

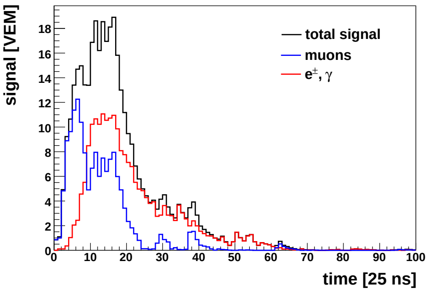

Average X_{max} Fluorescence Detector

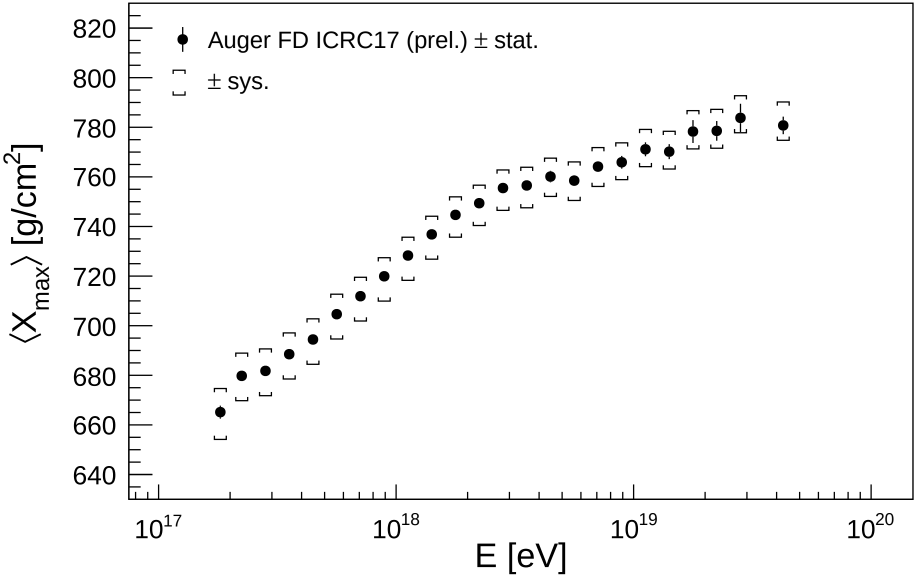

Average X_{max} Fluorescence Detector

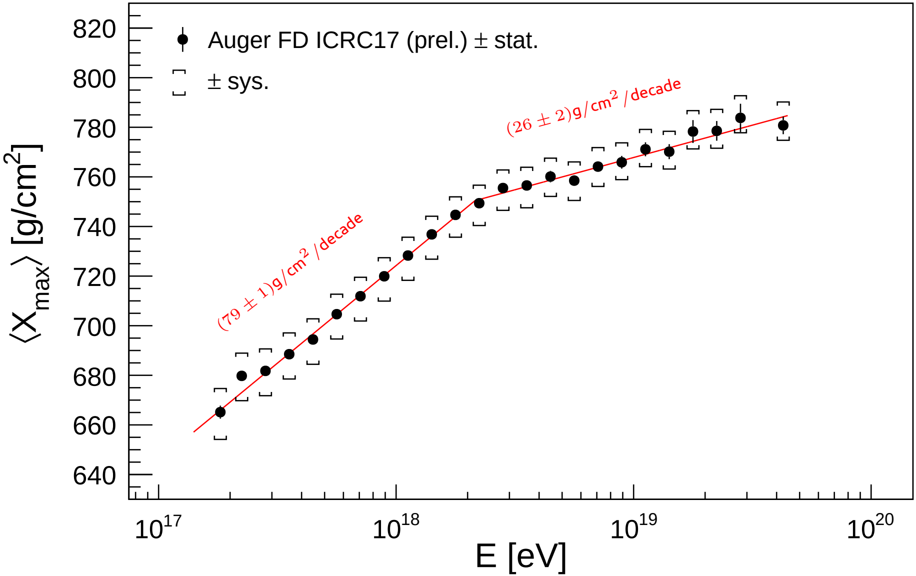

Average X_{max} Fluorescence and Surface Detector

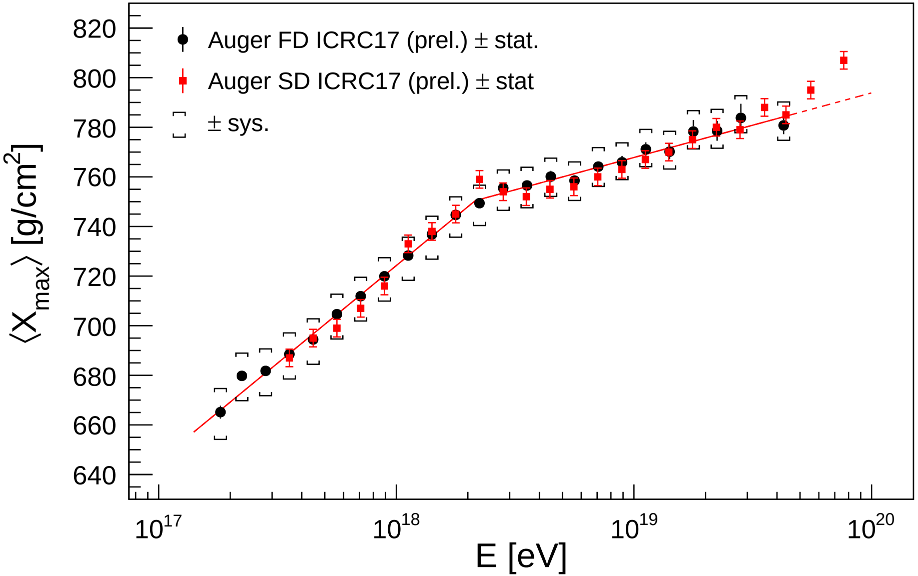

Standard Deviation of X_{max} Distribution

- $\sigma(X_{\text{max}})^2_A = \lambda^2_A + \sigma(X_{\text{max}} - X_{\text{first}})^2_A$
- $\sigma(X_{\text{max}})_p > \sigma(X_{\text{max}})_A > \sigma(X_{\text{max}})_p/\sqrt{A}$
- mixed composition:
  $\sigma(X_{\text{max}})^2 = \langle\sigma_i^2\rangle + \left(\left\langle\langle X_{\text{max}}\rangle_i^2\right\rangle - \langle X_{\text{max}}\rangle^2\right)$

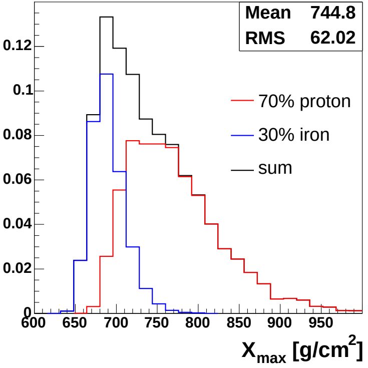

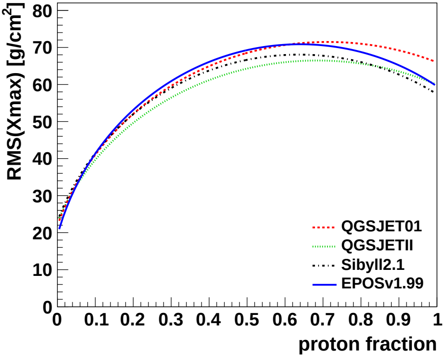

Standard Deviation of X_{max} Distribution (FD)

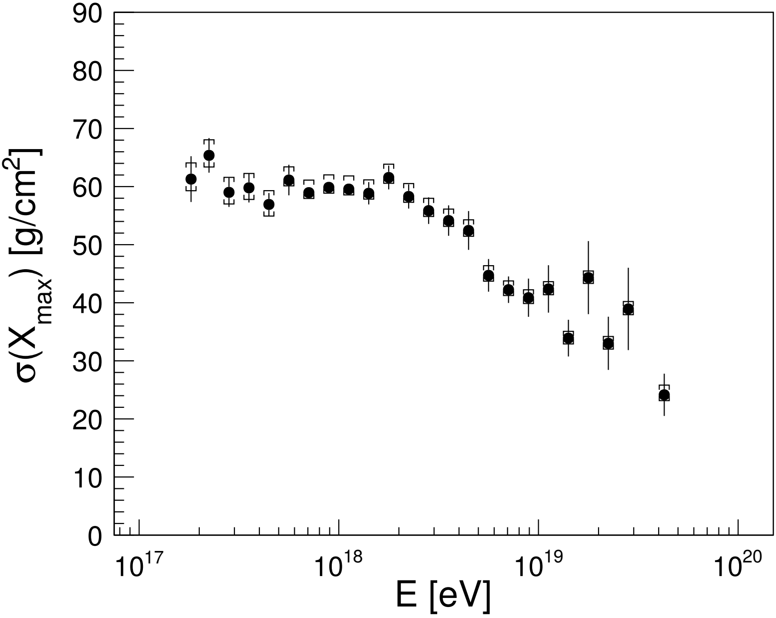

X_{max} Moments vs. Air Shower Simulations

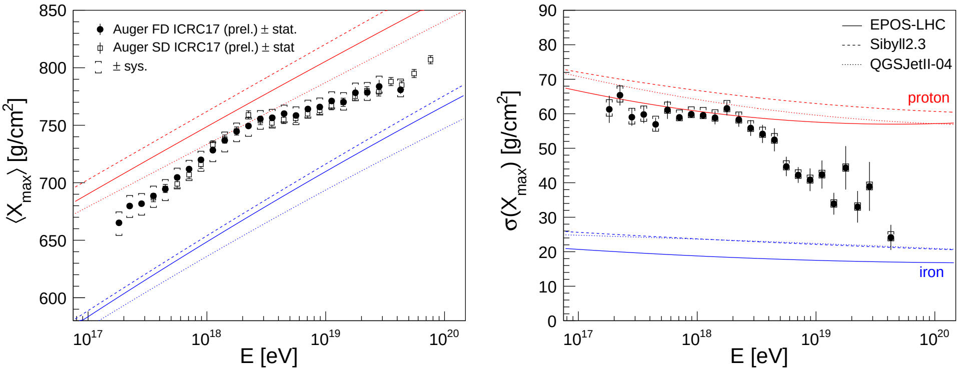

lines: air shower simulations using post-LHC hadronic interaction models

(p-He-N-Fe)-fit of X_{max} Distributions

FD data:

$\lg(E/\mathrm{eV}) = 17.2 \ldots 18.1$

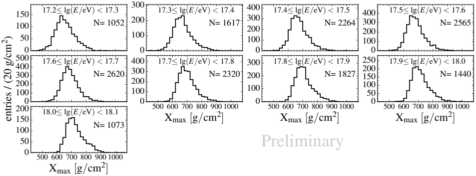

$\lg(E/\mathrm{eV}) = 17.8 \ldots > 19.5$

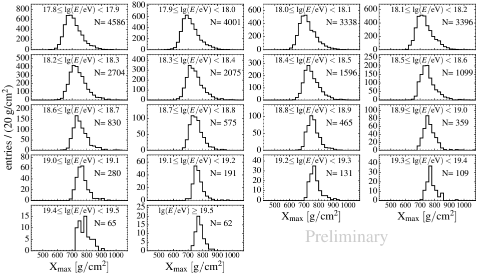

Examples of 4-component fit:

p He N Fe

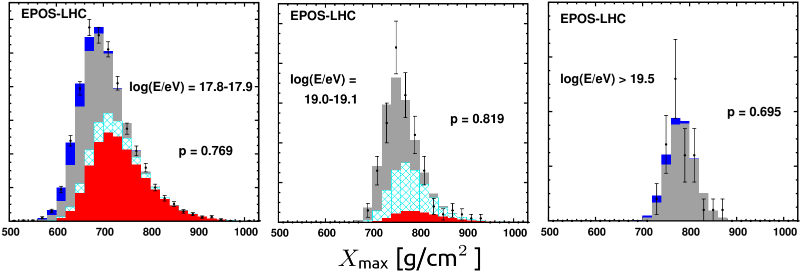

Composition Fractions

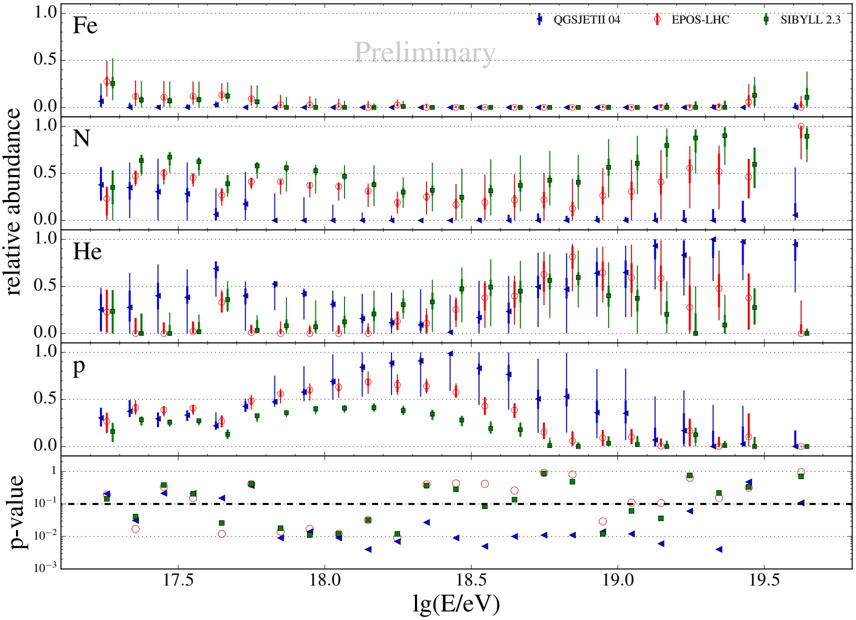

Combined Fit of Spectrum and X_{max} Distributions

rigidity-dependent cutoff at source: $E_{max} = R_{cut}\, Z$, power law injection $E^{-\gamma}$,
propagation with CRPropa3, Gilmore12 EBL, Dolag12 LSS

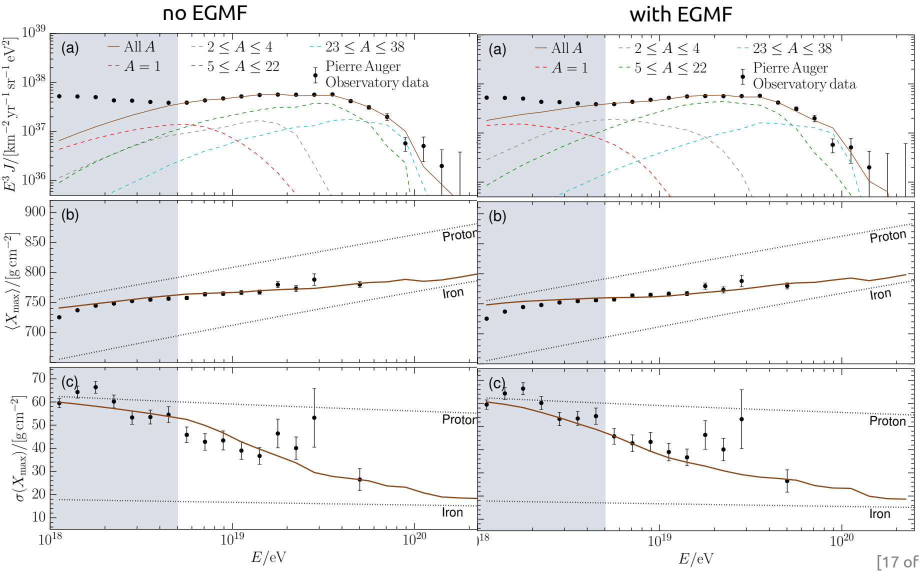

Combined Fit of Spectrum and X_{max} Distributions

rigidity-dependent cutoff at source: $E_{max} = R_{cut}\, Z$, power law injection $E^{-\gamma}$, propagation with CRPropa3, Gilmore12 EBL, Dolag12 LSS

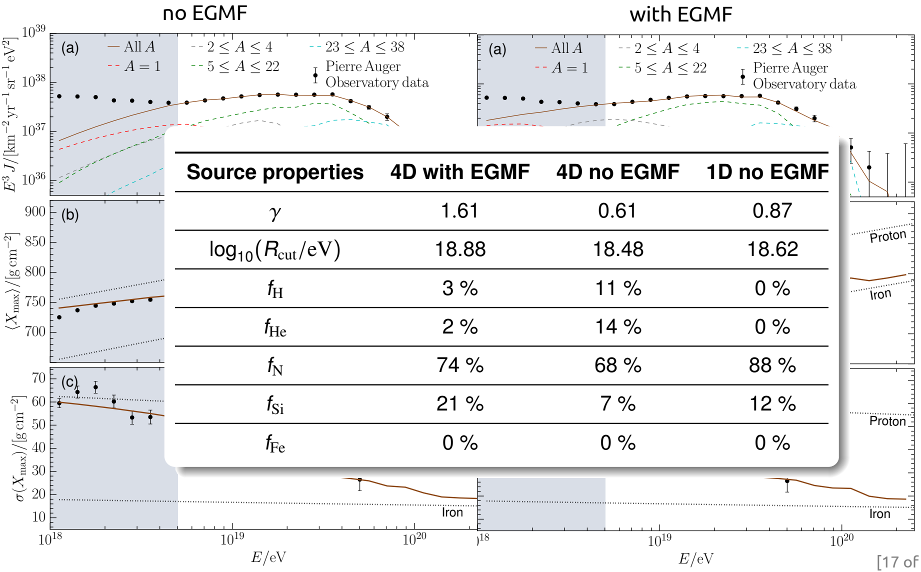

Source properties	4D with EGMF	4D no EGMF	1D no EGMF
γ	1.61	0.61	0.87
$\log_{10}(R_{cut}/\mathrm{eV})$	18.88	18.48	18.62
f_{H}	3 %	11 %	0 %
f_{He}	2 %	14 %	0 %
f_{N}	74 %	68 %	88 %
f_{Si}	21 %	7 %	12 %
f_{Fe}	0 %	0 %	0 %

Arrival Directions

- **Indication for Intermediate-scale Anisotropy**

  accepted by ApJ. Lett., arXiv:1801.06160

- **Observation of Large-scale Anisotropy**

  Science 357 (2017) 1266

Arrival Directions

- **Indication for Intermediate-scale Anisotropy**

  accepted by ApJ. Lett., arXiv:1801.06160

- **Observation of Large-scale Anisotropy**

  Science 357 (2017) 1266

Search for Intermediate-scale Anisotropies

Analysis Strategy:

- arrival directions of data, D
- sky model from source candidates, M_i

$M_i =$ (flux model) $\times$ (attenuation model) $\times$ (angular smearing) $\times$ (exposure)

- null hypothesis: isotropy M_0
- single population signal model:

$$M = (1 - \alpha)\, M_0 + \alpha\, M_i$$

- test statistics:
  - ratio of likelihoods of model-data comparison

    $$\mathrm{TS} = 2\log(P(D|M)/P(D|M_0))$$

    think $\Delta\chi^2$ of (isotropy + signal) vs. isotropy
  - p-value from Wilk's theorem: $p(\mathrm{TS}) = p_{\chi^2}(\mathrm{TS}, \Delta\mathrm{ndf})$
  - of large TS
    - M describes D much better than M_0
    - M_0 excluded at p (**not**: M "proven" at p)

UHECR Source Suspects

Swift-BAT 2MRS SBG γAGN ~~VCV~~

- *Swift*-BAT X-ray-selected galaxies, $D < 250$ Mpc, $\Phi > 1.3 \cdot 10^{-11} \frac{\text{erg}}{\text{cm}^2\ \text{s}}$, w : 14-195 keV
- 2MRS IR-selected galaxies, $D > 1$ Mpc, w : K-band
- SBG: 23 nearby starburst galaxies, $\Phi > 0.3$ Jy, w : radio at 1.4 GHz
- γAGN: 17 2FHL blazars and radio galaxies, $D < 250$ Mpc, w : γ-ray 50 GeV-2 TeV.

w : UHECR flux proxy, *Swift*-BAT and 2MRS previously tested (ApJ **804** (2015) 172), extragal. γ-ray sources γAGN and SBG.

Flux Attenuation (top: SBG, bottom: γAGN)

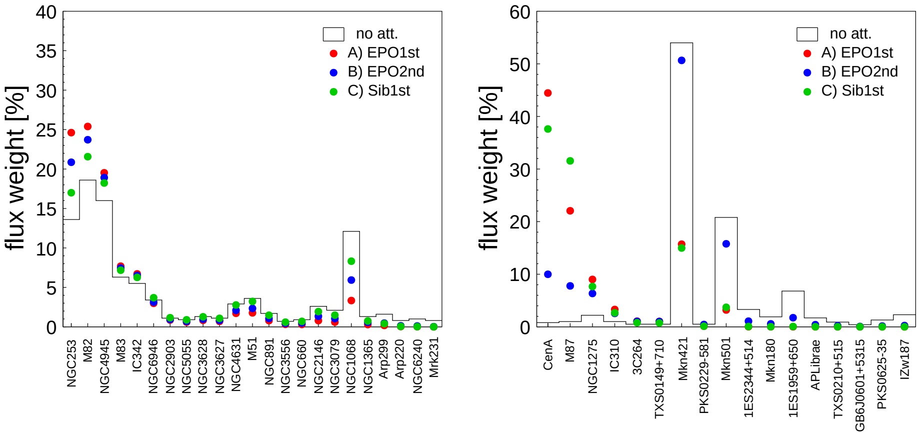

composition scenarios from Pierre Auger Coll., JCAP **1704** (2017) 038 + CRPropa3

name	$\lg(R_{\max}/\mathrm{V})$	f_p	f_He	f_N	f_Si	γ
EPO1st	18.68	0.000	0.673	0.281	0.046	0.96
EPO2nd	19.88	0.000	0.000	0.798	0.202	2.04
Sib1st	18.28	0.702	0.295	0.003	0.000	-1.50

Optimization: Signal Fraction and Angular Smearing

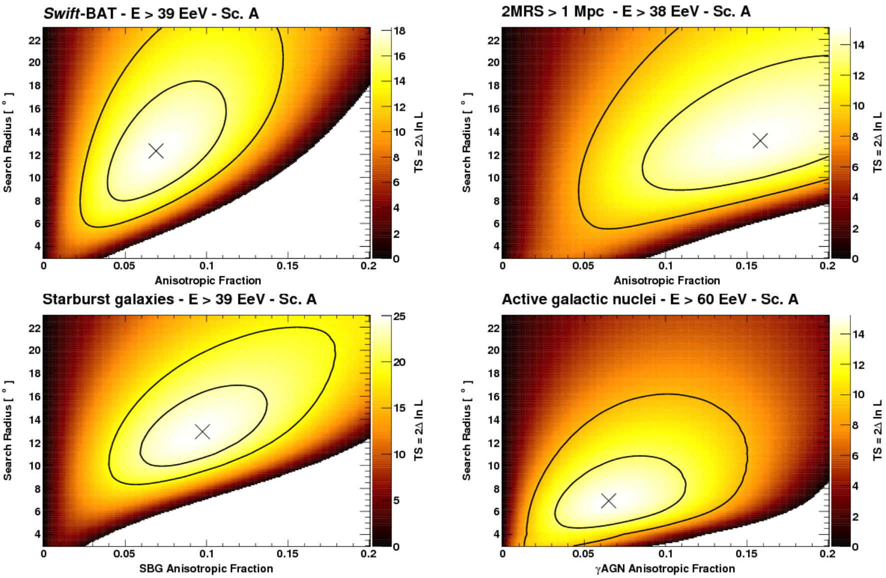

Sky Model (flux) × (attenuation model)$_A$ × (angular smearing), gal. coord.

Model Flux Map - *Swift*-BAT - E > 39 EeV - Sc. A

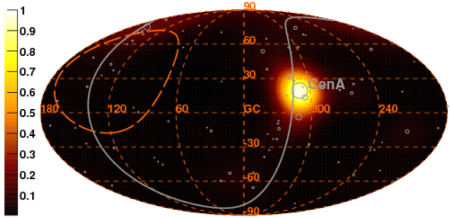

Model Flux Map - 2MRS > 1 Mpc - E > 38 EeV - Sc. A

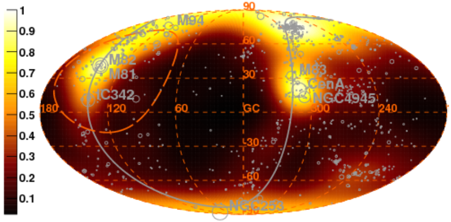

Model Flux Map - Starburst galaxies - E > 39 EeV - Sc. A

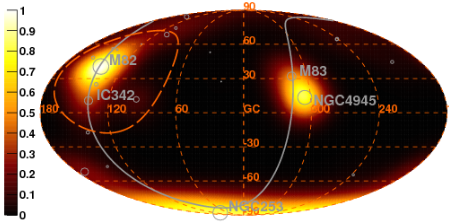

Model Flux Map - Active galactic nuclei - E > 60 EeV - Sc. A

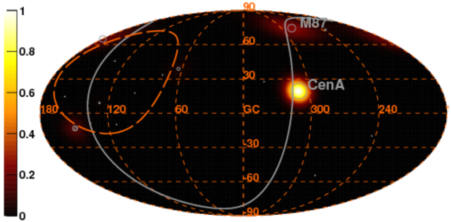

Sky Model (flux) × (attenuation model)$_A$ × (angular smearing), super-gal. coord.

Model Flux Map - *Swift*-BAT - E > 39 EeV - Sc. A

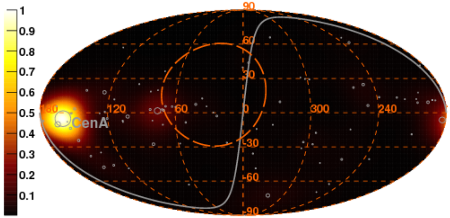

Model Flux Map - 2MRS > 1 Mpc - E > 38 EeV - Sc. A

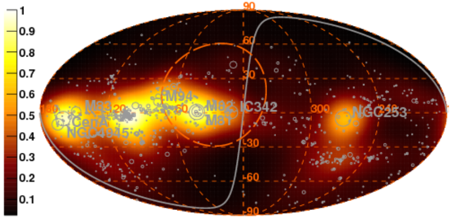

Model Flux Map - Starburst galaxies - E > 39 EeV - Sc. A

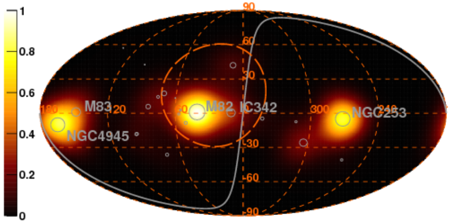

Model Flux Map - Active galactic nuclei - E > 60 EeV - Sc. A

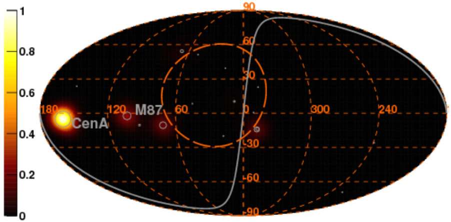

Sky Model (flux) $\times$ (attenuation model)$_B$ $\times$ (angular smearing), super-gal. coord.

Model Flux Map - *Swift*-BAT - E > 39 EeV - Sc. B

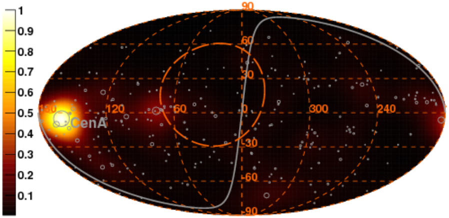

Model Flux Map - 2MRS > 1 Mpc - E > 38 EeV - Sc. B

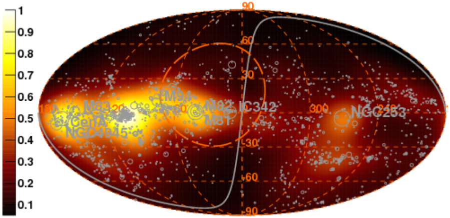

Model Flux Map - Starburst galaxies - E > 39 EeV - Sc. B

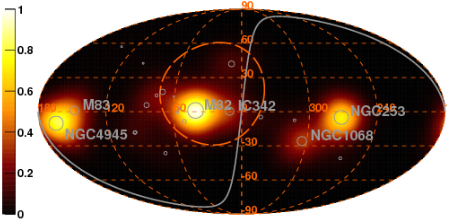

Model Flux Map - Active galactic nuclei - E > 60 EeV - Sc. B

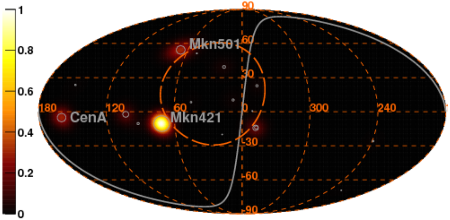

Test Statistics vs. Energy

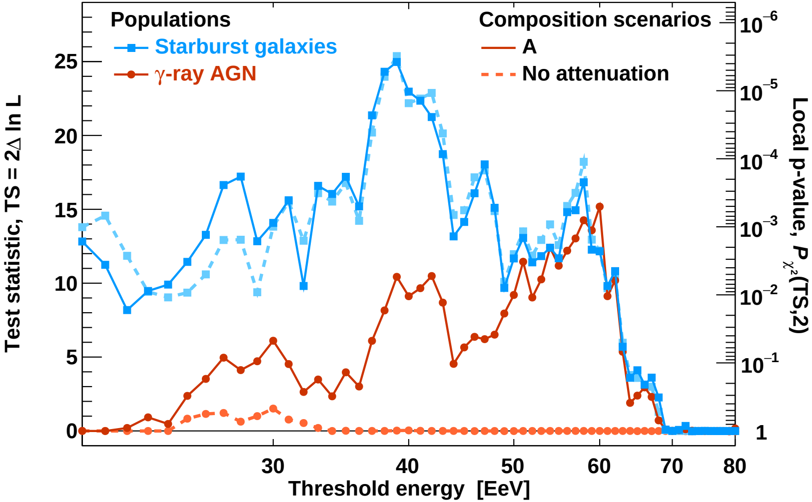

starburst model fits data better than isotropy, significance of 4 σ^*.

* $P_{\chi^2}(\text{TS}, 2)$ penalized for energy scan

Test Statistics vs. Energy

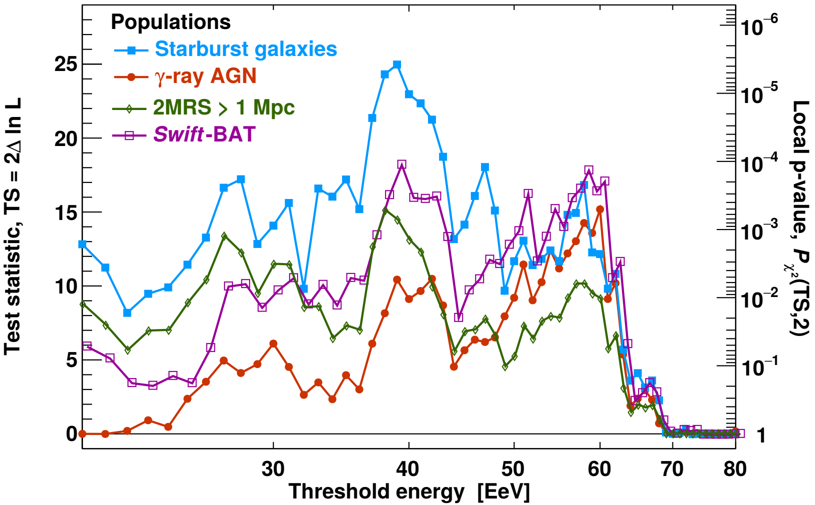

starburst model fits data better than isotropy, significance of 4 σ^*.

$^*\ P_{\chi^2}(\mathrm{TS},\ 2)$ penalized for energy scan

Detailed View of Sky Models

Test hypothesis	Null hypothesis	Threshold energy[a]	TS	Local p-value $\mathcal{P}_{\chi^2}(\mathrm{TS}, 2)$	Post-trial p-value	1-sided significance	AGN/other fraction	SBG fraction	Search radius
SBG + ISO	ISO	39 EeV	24.9	3.8×10^{-6}	3.6×10^{-5}	$4.0\,\sigma$	N/A	9.7 %	12.9°
γAGN + SBG + ISO	γAGN + ISO	39 EeV	14.7	N/A	1.3×10^{-4}	$3.7\,\sigma$	0.7 %	8.7 %	12.5°
γAGN + ISO	ISO	60 EeV	15.2	5.1×10^{-4}	3.1×10^{-3}	$2.7\,\sigma$	6.7 %	N/A	6.9°
γAGN + SBG + ISO	SBG + ISO	60 EeV	3.0	N/A	0.08	$1.4\,\sigma$	6.8 %	0.0 %[b]	7.0°
Swift-BAT + ISO	ISO	39 EeV	18.2	1.1×10^{-4}	8.0×10^{-4}	$3.2\,\sigma$	6.9 %	N/A	12.3°
Swift-BAT + SBG + ISO	*Swift*-BAT + ISO	39 EeV	7.8	N/A	5.1×10^{-3}	$2.6\,\sigma$	2.8 %	7.1 %	12.6°
2MRS + ISO	ISO	38 EeV	15.1	5.2×10^{-4}	3.3×10^{-3}	$2.7\,\sigma$	15.8 %	N/A	13.2°
2MRS + SBG + ISO	2MRS + ISO	39 EeV	10.4	N/A	1.3×10^{-3}	$3.0\,\sigma$	1.1 %	8.9 %	12.6°

[a] For composite model studies, no scan over the threshold energy is performed.

[b] Maximum TS reached at the boundary of the parameter space.

ISO: isotropic model.

Data vs. Model, SBG and γAGN (gal. coord.)

top: starburst galaxies

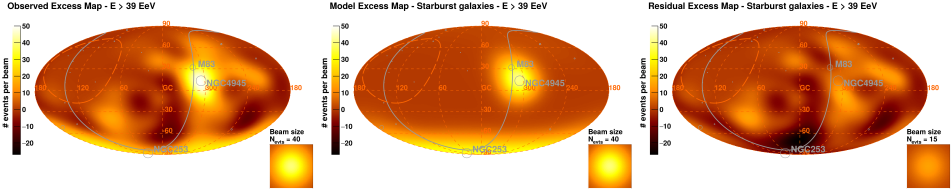

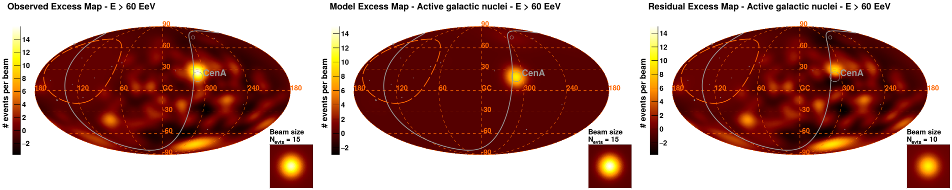

bottom: γAGN

Arrival Directions

- Indication for Intermediate-scale Anisotropy

  accepted by ApJ. Lett., arXiv:1801.06160

- **Observation of Large-scale Anisotropy**

  Science 357 (2017) 1266

Observation of Dipolar anisotropy above 8 EeV

Harmonic analysis in right ascension α

E [EeV]	events	amplitude r	phase [deg.]	$P(\geq r)$
4-8	81701	$0.005^{+0.006}_{-0.002}$	80 ± 60	0.60
> 8	32187	$0.047^{+0.008}_{-0.007}$	100 ± 10	2.6×10^{-8}

significant modulation at 5.2 σ (5.6σ before penalization for energy bins explored)

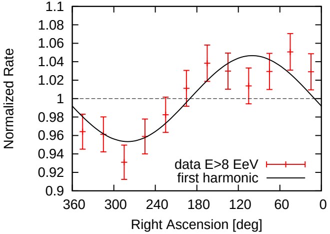

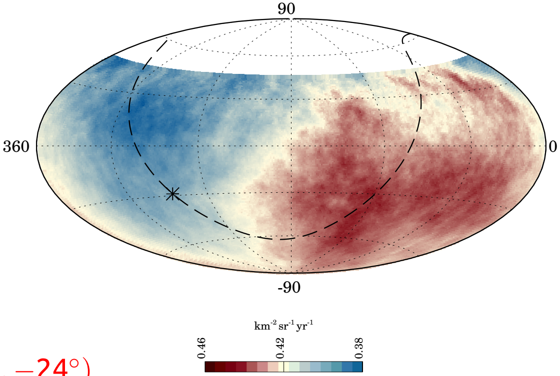

3-d dipole above 8 EeV:

$(6.5^{+1.3}_{-0.9})$% at $(\alpha, \delta) = (100°, -24°)$

Dipole in Galactic Coordinates

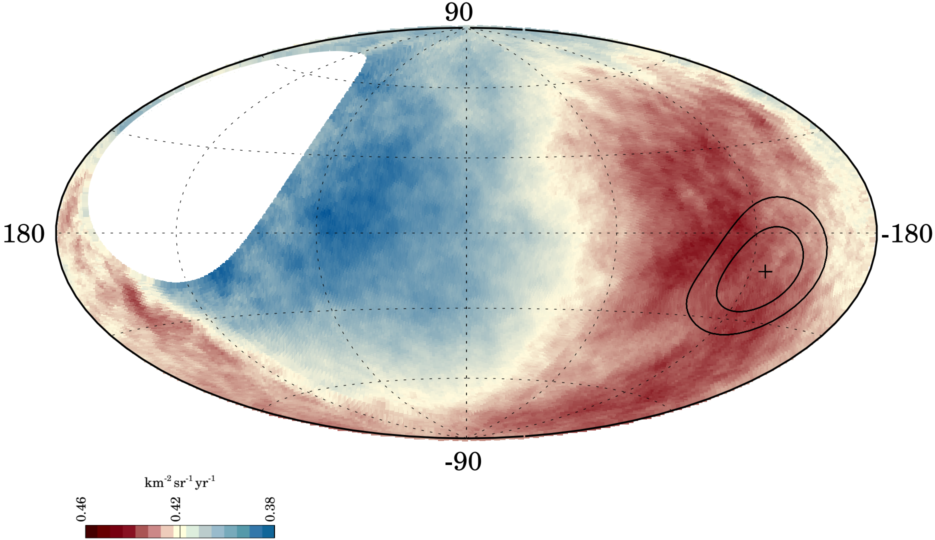

Dipole in Galactic Coordinates

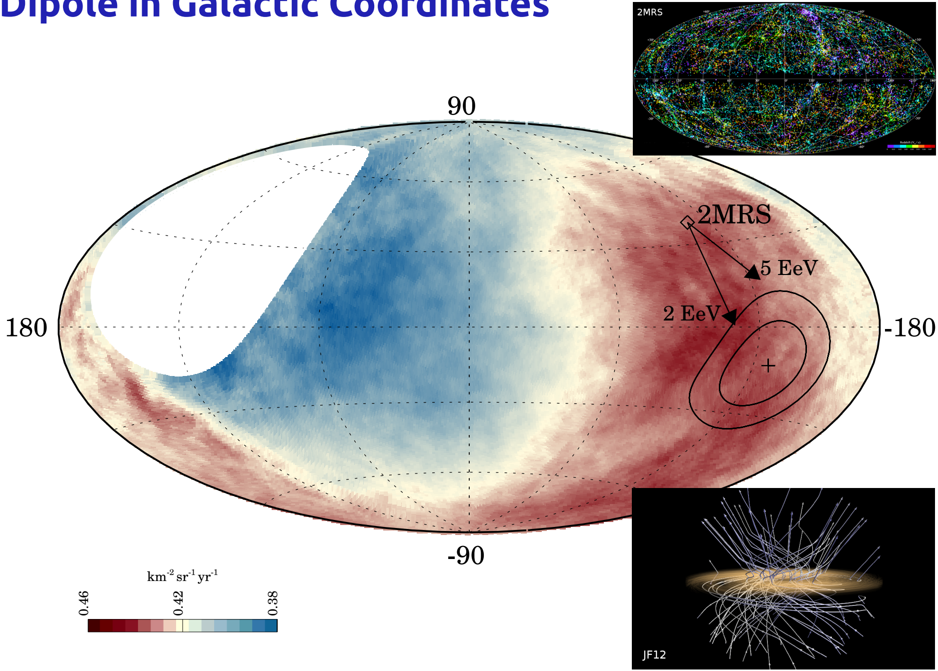

Summary and Outlook

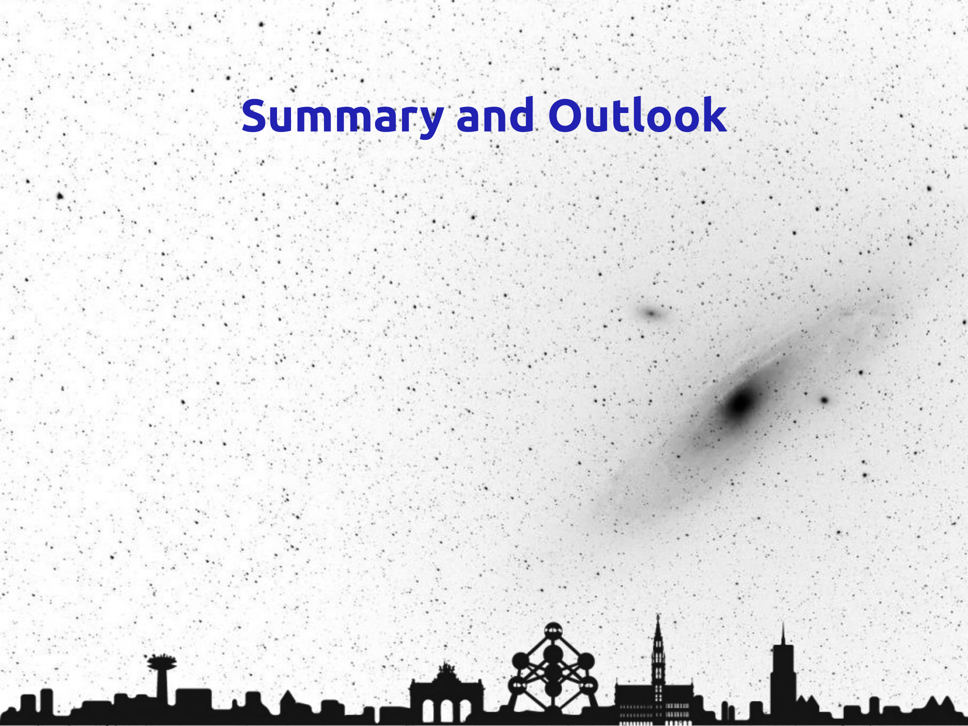

Results

spectrum, composition, secondaries:

- high-exposure study of UHE flux
  $\rightarrow$ strong flux suppression
- FD/SD composition studies
  $\rightarrow$ light composition at ankle
  $\rightarrow$ mixed composition at UHE
  $\rightarrow$ Galactic Fe around $10^{17.2}$ eV?
- constraints on p-dominated sources via ν/γ
- compatible with rigidity-dependent E_{max}

hadronic interactions:

- standard UHE cross section
- muon deficit in models

arrival directions:

- indication for intermediate-scale anisotropy
- observation of dipolar anisotropy

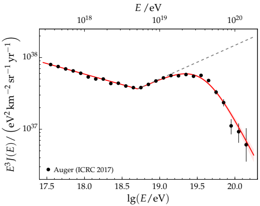

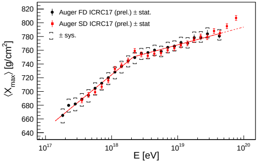

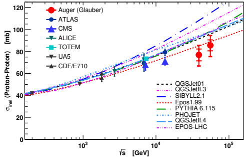

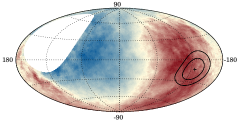

Open Questions

- Origin of the flux suppression?
- Proton fraction at UHE?
- Rigidity-dependence of anisotropies?
- Hadronic physics above $\sqrt{s} = 140$ TeV?

need large-exposure detector with composition sensitivity!

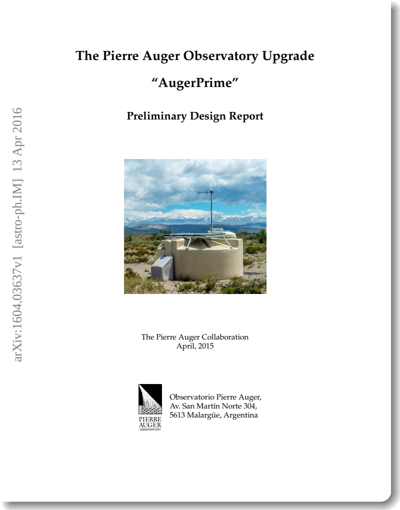
arXiv:1604.03637v1 [astro-ph.IM] 13 Apr 2016

The Pierre Auger Observatory Upgrade

"AugerPrime"

Preliminary Design Report

The Pierre Auger Collaboration
April, 2015

PIERRE AUGER OBSERVATORY

Observatorio Pierre Auger,
Av. San Martín Norte 304,
5613 Malargüe, Argentina

Detector Upgrades for AugerPrime

- 3.8 m^2 scintillators (SSD) on each 1500-m array station
- upgrade of station electronics
- additional small PMT to increase dynamic range
- buried muon counters in 750-m array (AMIGA)
- increased FD uptime

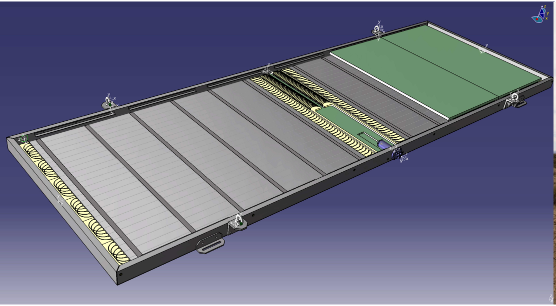

Expected Performance of AugerPrime

X_{max} determination:

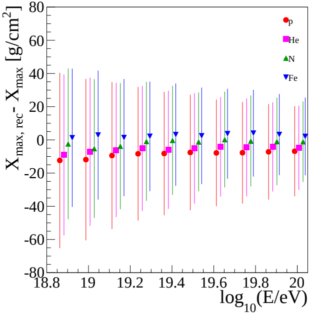

muon determination:

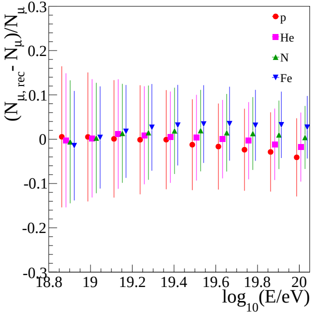

high- vs. low-R_{cut} scenario:

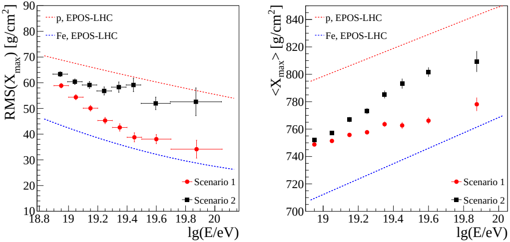

low-Z particle astronomy:

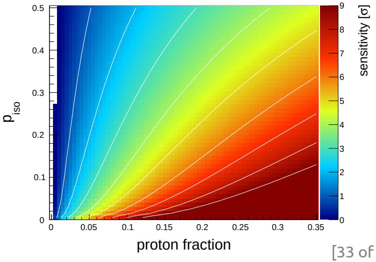

AugerPrime Engineering Array

AugerPrime Engineering Array

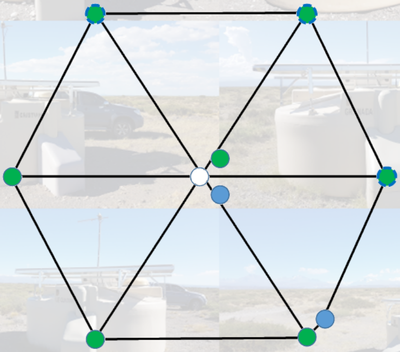

1500 m hexagon

- SSD w PMT-ISEG base
- SSD w PMT-passive base
- SSD w SiPM
- WCD w/o SSD

quadruplet in 750 m array

AugerPrime Engineering Array

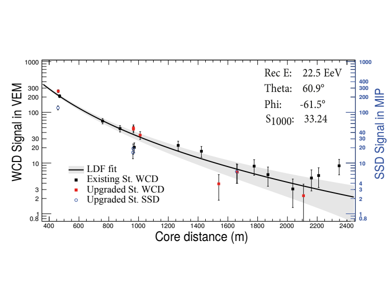

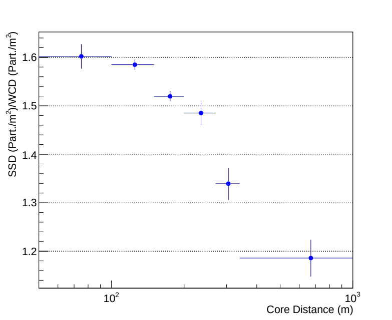

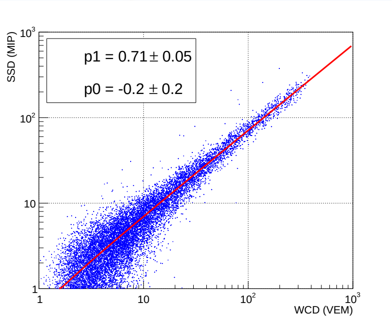

- design finalized and tested
- 70% of funding secured
- finish construction by 2019
- data taking $\gtrsim$ 2025

Thanks!